The fabrication of an eccentric three-core fiber and its application as a twist sensor

Pingsheng Xue, Qiang Liu, Qiang Wu and Richard Fu.

***Abstract*—The fabrication and application for twist sensing of an eccentric three-core fiber were demonstrated. The fiber was made by stack-and-draw technique, in which silica rods and core canes were put in a tube and drawn on a fiber drawing tower. Three cores formed a Mach-Zehnder interferometer, where the lights transmitted in the three cores interfered with each other, resulted in the formation of envelopes on spectrum. Because two of the cores were off axis, phase differences among the cores varied with twist due to different stretches on each core, which caused shift of the spectral envelopes of the interference signal. Wide range twist measurement can be realized with relatively high sensitivity by tracking lower dips of the envelopes. Experimental results revealed that the dips shift quadratically with twist angle, which means that the sensitivity increases with twist. The compensation of temperature influence was also implemented by inscribing a Bragg grating on one of the cores with femtosecond laser. Because the fiber can be mass-produced, it is suitable for twist sensing in practical application for its low cost.**

***Index Terms*—Fiber sensor; Twist; Three-core fiber; Mach-Zehnder interferometer.**

I. Introduction

FIBER sensors [1]-[4] have more advantages compared with traditional sensors. They are flexible, light weight, quick in response, immure to electromagnetic interference and corrosion, and have been widely investigated for structural health monitoring in fields like aircraft, ground deformation, landslide, and ground fissure [5]-[7]. Twist sensing is significant in engineering, industry, architecture etc. to monitor the parameters of mechanical parts or building structures. So far, most fiber twist sensors are based on fiber gratings [8]-[13], or fiber loop mirrors (Sagnac interferometers) [14]-[16].

In [8], X. Chen et al. utilized a fiber Bragg grating (FBG) with 81° tilted structure to measure twist, the sensitivity was 14.3 W/(rad/m). In [9], Y. Lu et al. also used a tilt FBG for twist sensing, and they discussed the polarization dependence of the sensor, sensitivity of 0.299 dB/° was obtained in measuring range of 180°. A method to measure twist by analyzing polarization dependent loss of FBG was presented in [10]. C. Shen et al. realized a twist sensor based on surface plasmon resonance of an Au coated FBG [11]. R. Gao et al. introduced phase shift helical long period fiber grating and realized temperature insensitive twist sensor, the sensitivity was up to 1.959 nm/(rad/m) [12]. Helical long period grating for twist and temperature sensing was also presented in [13]; the advantage of helical grating is the capability of twist direction discrimination by using the fact that twist influences the grating period directly. However, the fabrications of tilt or helical gratings mentioned above are relatively complicated. In fact, the grating structures are all post-processed on a traditional fiber. In addition, because the processing methods are usually heating the fiber with laser or flame, the fiber becomes extremely fragile afterwards, which is a problem to be utilized in practice.

Twist sensor based on photonic crystal fiber Sagnac interferometer was designed in [14], having sensitivity of 1 nm/°. In [15], a compact Sagnac loop based on a microfiber coupler for twist sensing with sensitivity of 0.9 nm/° was designed by Y. Chen et al. Temperature and torsion simultaneous sensing was presented in [16]. The fiber loop configurations are large, which is not convenient enough in reality. B. Huang et al. realized a temperature and strain independent twist sensor in [18] base on a Lyot filter, whose structure was easier to configure. Meanwhile, some of the related works are based on intensity demodulation, which means measuring twist by observing the varying light intensities, however it can be easily influenced by fluctuation of the light source, by contrast observing the wavelengths of dips is more stable since the intensity fluctuation does not affect the dip wavelengths.

We introduce the fabrication of an asymmetric and eccentric three-core fiber (3CF) and its application for twist sensing in this paper. The 3CF which was sensitive to twist deformation was configured to a Mach-Zehnder interferometer (MZI), the beams in three optical paths interfered with each other and resulted in forming envelopes on spectrum. Twist sensing was realized by observing the shifts of spectrum envelopes. The twist sensing MZI showed relatively high sensitivity and wide measurement range, the reversibility was satisfactory, those characteristics make the device competitive in the sensing field. Temperature influence was also considered and could be compensated by inscribing an FBG on one of the cores. The fiber has good mechanical strength and can be produced massively, it is also cheap. With the advantages, this typical fiber is suitable for twist measurement to monitor the health of

Manuscript received ******; revised ******.This research was funded by the National Natural Science Foundation of China (Grant No. 51907017), the Key Science and Technology Research Projects of Higher Education Institutions in Hebei Province of China (Grant No. ZD2019304), Hebei Natural Science Foundation (Grant No. F2020501040), the Fundamental Research Funds for the Central Universities of China (Grant No. N2123012). (Corresponding author: Qiang Liu.)

Pingsheng Xue and Qiang Liu are with the College of Information Science and Engineering, Northeastern University, Shenyang 110819, China. School of Control Engineering, Northeastern University at Qinhuangdao, Qinhuangdao 066004, China and also with the Hebei Key Laboratory of Micro-Nano Precision Optical Sensing and Measurement Technology, Qinhuangdao 066004, China (e-mail: e-mail: 1901906@stu.neu.edu.cn; liuqiang@neuq.edu.cn).

Qiang Wu and Richard Fu are with the Faculty of Engineering and Environment, Northumbria University, Newcastle upon Tyne NE1 8ST, U.K. (e-mail: qiang.wu@northumbria.ac.uk; richard.fu@northumbria.ac.uk;

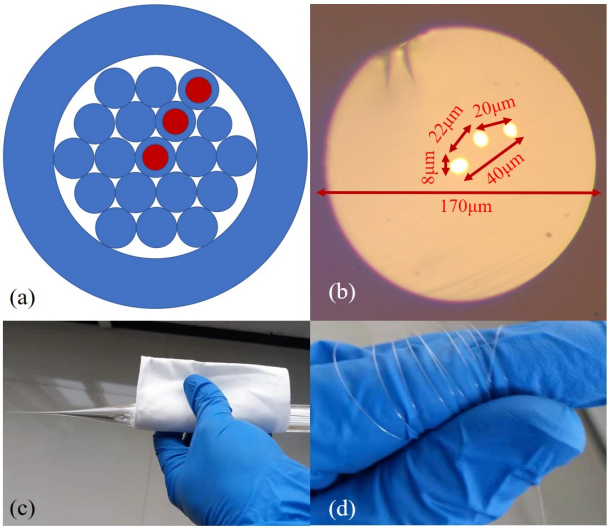

Fig. 1. (a) Silica rods and cores (red) alignment of the stacked preform. (b) Cross section of the fiber, the sizes and distances between cores are as labeled. (c) The preform after drawing. (d) Drawn fiber, showed good mechanical strength when annealed properly. Hundred meters of the fiber was produced.

bridges, dams buildings, propellers, shafts and pipes in civil, mechanical and industrial engineering.

II. Fabrication of the Fiber and Sensing Principle

The normal manufacturing technique like Chemical Vapor Deposition (CVD) or Modified CVD (MCVD) method usually cannot create eccentric or asymmetry fiber preforms. At present, most common ways to fabricate fiber preforms with unusual structures are drilling holes [19] and stack-and-draw method [20], [21]. By settling core rods in the drilled holes, multi-core or eccentric core fibers can be produced, the shape and structure are more stable during drawing with drilling hole method. Stack-and-draw technique is often used to fabricate photonic crystal fiber (PCF), while this method is also competent to produce multi-core or eccentric core fiber. Compared with drilling hole method whose drilling depths on preforms are usually less than a dozen centimeters, the preforms in stack-and-draw method can be quite longer, which means it can produce much longer fibers at one time with this method.

The asymmetry three-core fiber used in our experiment was fabricated by stack-and-draw technique. In order to have a clear and low loss spectrum, we designed the diameter of cores to be 9 μm, which is the same size of a standard single-mode fiber (SMF), and to optimize interference the distances between adjacent cores were designed to be 20-30 μm. Firstly a multi-mode fiber (MMF) preform (core refractive index ~1.465) was drawn to canes with a diameter of ~2.3 mm, these canes play the role of cores in the following asymmetry three-core fiber. The three core canes and 16 silica rods also in ~2.3 mm diameter were stacked in hexagon shape in a silica tube with 12 mm inner and 20 mm outer diameter. The cores and rods alignment is shown in Fig. 1(a). With the settings above, fibers that meet the requirements can be produced. Before drawing on the tower, the stacked preform was set

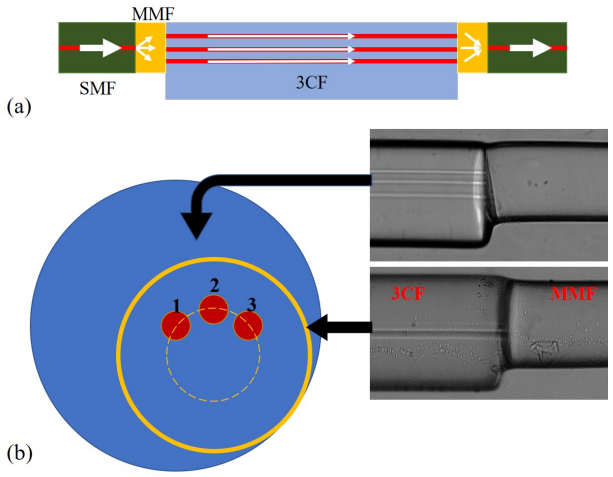

Fig. 2. (a) Schematic of the MZI, small sections of MMF were spliced between SMF and 3CF. (b) The MMF and 3CF were spliced with an offset to make intensities among each core are approximately the same, so that the contrast of interference spectrum can be improved.

on an oxy-hydrogen flame lathe to melt and seal the bottom end. During drawing, the furnace temperature was 1800 °C, feeding and drawing speed were as low as 0.05 mm/min and 0.8 m/min so the drawn fiber could anneal slowly, otherwise the fiber would be very fragile if there were residual thermal stress. Coating layer was also introduced to ensure mechanical strength. The cross section of drawn fiber is shown in Fig. 1(b). Though slightly displaced after drawing, the three cores were in good conditions. The diameter of the fiber is 170 μm, core diameters are 8 μm, distances between the cores are labeled in Fig. 1(b), core 1 is in the center. The cores are far enough from each other so the coupling between waveguides are weak and negligible.

The 3CF can be embedded in an MZI. The MZI output intensity is expressed as [22], [23]:

$$I = I_1 + I_2 + 2\sqrt{I_1 I_2}\cos\varphi \tag{1}$$

In which:

$$\varphi = 2\pi\left(L_1 n_1 - L_2 n_2\right)/\lambda$$

I_1, I_2 are intensities of two beams and φ is the phase difference, L_1, L_2 and n_1, n_2 are the corresponding lengths and refractive indices. The destructive interference occurs when $\varphi = (2m+1)\pi$ and dips can be observed on the optical spectrum analyzer (OSA). Dip intervals, or free spectrum ranges (FSR) are calculated by:

$$FSR = \lambda^2/\left(L_1 n_1 - L_2 n_2\right) \tag{2}$$

To incident light into the three cores from leading in SMF, a short section of MMF (~1 mm) was spliced between the 3CF and SMF (Fig. 2(a)), it is worth mentioning that in order to have larger extinction ratio of the interference dip and make the spectrum more obvious, the intensities of light transmitted in three cores should be similar. On the splicing end faces, the distances from cores to the center of the MMF should be as equal as possible. So the 3CF and MMF were spliced with an

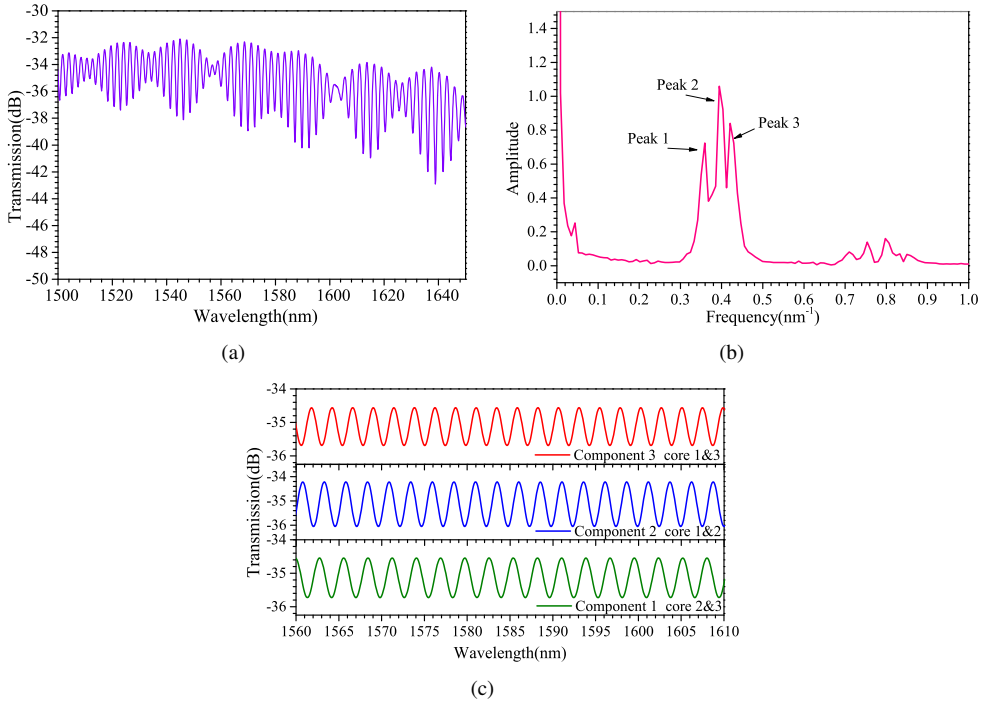

Fig. 3. (a) Output spectrum of the 3CF MZI, multiple interferences formed envelopes. (b) FFT of the spectrum, three main peaks show the spectrum is consisted of three different components. (c) Three components extracted by bandpass filter. (Top: interference between core 1 and 3; middle: core 1 and 2; bottom: core 2 and 3).

offset, as indicated in Fig. 2(b). The 170 μm large diameter allows more overlaps on the end face with 125 μm MMF, which makes sure the splicing point tough enough. The precise offset splicing can be realized by the polarization-maintain fiber splicer with rotation motors (FSM-100P+, Fujikura).

When the 3CF is straight and suffers no twist or bending, the optical paths in each core are equal and no interference will occur. To induce phase difference among the beams in each path and form Mach-Zehnder interference, 1.8 m of 3CF was wound into several laps, phase differences occurred among each path because the stretches on each core are different due to the off-axis of core 2 and 3. The fiber was connected to a broadband light source and the spectrum was observed with an OSA. The spectrum of the MZI which is shown in Fig. 3(a) consists of multiple components and forms envelope. Each two of the three paths interfere with each other, so the interference spectrum should mainly have three components (which are interference between core 1 and 2, 2 and 3, 1 and 3). There are three main peaks at 0.359, 0.394 and 0.420 nm^{-1} in the Fast Fourier transform (FFT, sampling interval 0.1) spectrum (Fig. 3(b)), which corresponds to those three interference components. Then the interference spectrum was filtered by band-pass filter with passing band of 0.3585-0.3595, 0.3935-0.3945 and 0.4195-0.4205 to extract each component, which is shown in Fig. 3(c). The top in Fig. 3(c) has smallest FSR, according to equation (2), it is the interference between core 1 and core 3, in which the optical path difference is the largest because core 1 suffers the least stretches caused by deformation and core 3 suffers the most; the middle shows the interference between core 1 and 2, and the bottom in Fig. 3(c) which has the largest FSR, is the interference between core 2 and 3, among which the optical path difference is the smallest. The output spectrum is the sum of three interferences. Then the output intensity of this 3CF MZI can be expressed as:

$$I = 2\Big(I_1 + I_2 + I_3 + \sqrt{I_1 I_2}\cos\varphi_{12} + \sqrt{I_2 I_3}\cos\varphi_{23} + \sqrt{I_1 I_3}\cos\varphi_{13}\Big) \tag{3}$$

I_1, I_2, I_3 and φ_{12}, φ_{23}, φ_{13} are intensities transmitted in each core and phase differences among them respectively, where:

$$\varphi_{12} = 2\pi\left[(n+\Delta n)l_2 - nl\right]/\lambda, \quad l_2 = \sqrt{(r_2\theta)^2 + l^2};$$

$$\varphi_{13} = 2\pi\left[(n+\Delta n)l_3 - nl\right]/\lambda, \quad l_3 = \sqrt{(r_3\theta)^2 + l^2};$$

$$\varphi_{23} = 2\pi\left[(n+\Delta n)l_3 - (n+\Delta n)l_2\right]/\lambda;$$

$$\Delta n = pn\varepsilon;$$

in which, p is the effective photoelastic constants, $\varepsilon = \Delta l/l$, l represents fiber length, Δl is deformation length of the related core, r is the distance from the related core to the fiber center, θ is twist angle. Since l is much larger than $r\theta$, and if we neglect Δn, which is tiny, $d\varphi/d\theta$ or $d\lambda/d\theta$ which represents the sensitivity of dips shift can be considered approximately

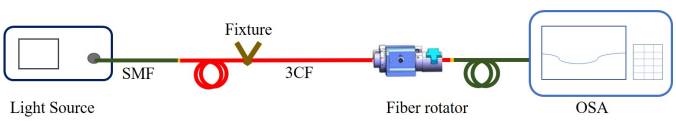

Fig. 4. Schematic of the twist sensing setup.

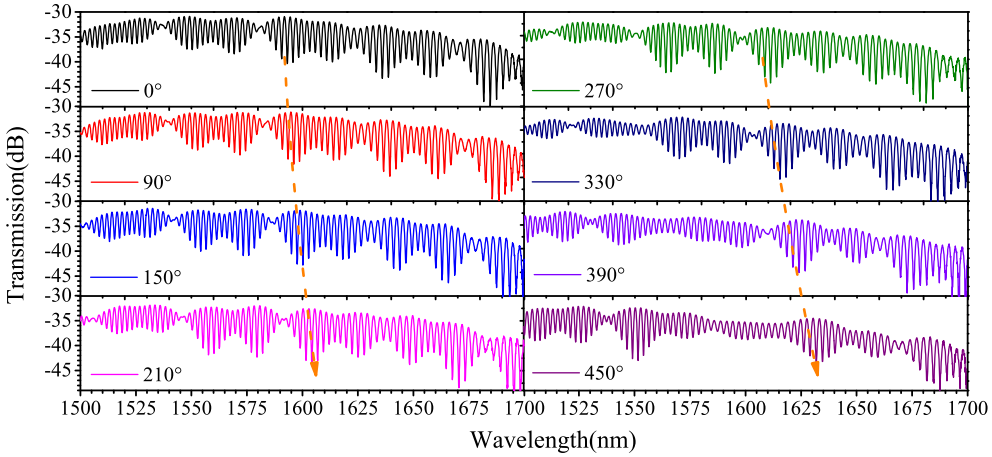

Fig. 5. The envelopes continuing red shift as the fiber suffers twist.

proportional to θ, that means the sensitivity increases with twist angle, and the dips shift response to θ is near quadratic. The envelope shift is the amplification of individual dip shift by a constant concerned with the FSRs, it will also shift quadratically with twist angle.

III. Results and Discussion

A. Twist sensing characteristics.

This 3CF can be applied for twist measurement. Experiment setup is shown in Fig. 4. The 3CF was 1.8 m, we coiled the fiber 5 rounds in diameters of 6 cm at one end to induce phase difference among three cores initially in order to form interference spectrum on the OSA. The distance between fixture and fiber rotator was 0.5 m. Leading out SMF was long enough so the influence of twist on SMF can be neglected. When twist was applied by rotating the fiber rotator, since core 1 is on the center axis of the fiber, it will not suffer much stretch, while core 2 will suffer more and core 3 the most stretch because of their eccentricities. The phase differences among these cores accumulate with twist angle, and causes three interference components shift asynchronously, sensitivity is amplified in this way. When the fiber was twisted to one side continuously, both the dips and the envelope red shifted. As it is shown in Fig. 5, envelope shift was marked. The shift was not obvious when twist angle was less than 90°, while the red shift of the envelope became more sensitive as twist increased. The lower envelope was outlined and the shift of its dip wavelengths were tracked as twist angle varied (Fig. 6(a)). When the fiber was twisted to the other direction, the envelope still red shifted and the responses to both directions were approximately the same. We chose three adjacent lower envelope dips initially at 1593.3 nm, 1569.2 nm and 1548.2 nm and tracked their shifts. The dip wavelengths shifts of the lower envelope versus twist angles are plotted in Fig. 6(b), the response to both twisting directions were symmetrical. The dots conform to quadratic functions which was consistent with our analysis. Repeated tests were carried out for 4 times and the dots for polynomial curve fitting were the average of 4 times data. The fitted equations are labeled, their colors

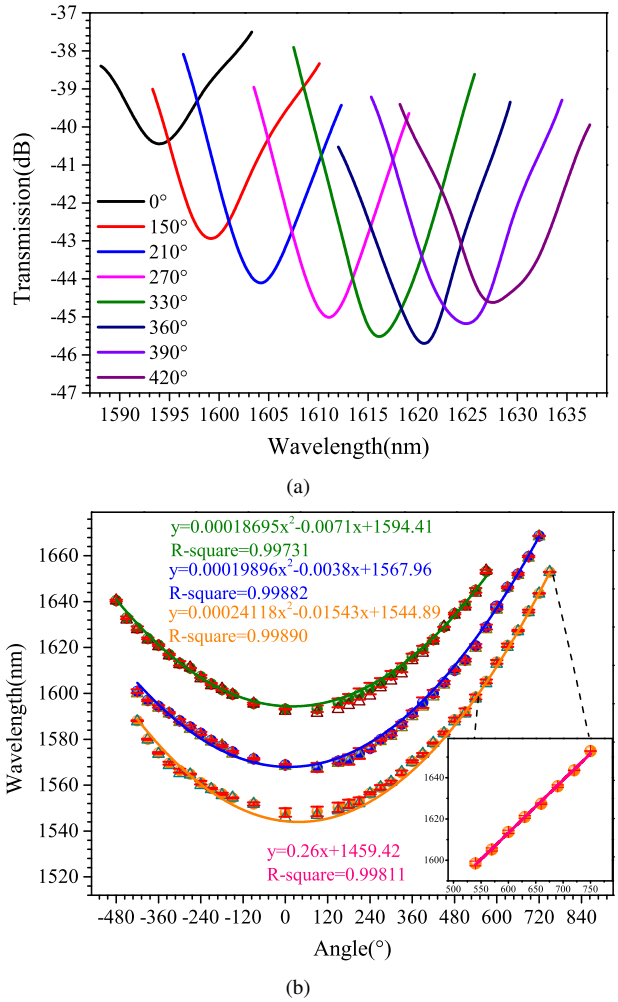

Fig. 6. (a) The lower envelopes were outlined and tracked as twist varying. (b) The relation between dip wavelengths of the lower envelope and twist angle, the envelopes shifts are symmetrical when the fiber was twisted to both directions. (Inset: linear fitting in range from 540° to 720°)

correspond to the curves, R-squares are as high as 0.99731, 0.99882 and 0.99890. Standard errors among repeated tests

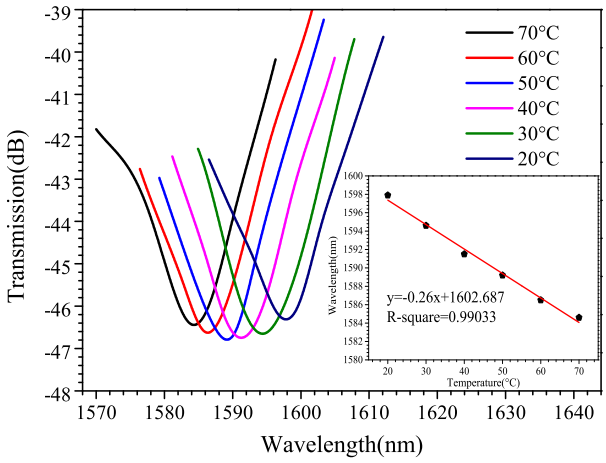

Fig. 7. The temperature influence on the envelope shift (outline of the lower envelope), (Inset: linear fitting of the relation between dip wavelengths of the lower envelope and temperature.)

were calculated and shown as error bars in the figure, and we may conclude from the error bars that the repeatability was satisfactory. Reverse response tests were also carried out and plotted as hollow triangle dots in Fig. 6(b). Hysteresis was negligible. The axes of symmetry of the fitted parabolas should be at x = 0 (no first power term of the polynomial) ideally, however tiny error exists in the results. The fiber tended to slip on the fixture as twist accumulated, which was mainly one of the sources of error. The spectrum would keep shifting if the twist further increased, however we stopped at 720° for the same reason. From 540° to 720°, the shift can be considered linear since the R-square for fitting was as high as 0.99811, the inset of Fig. 6(b) plots the linear fitted line, the slope indicates the sensitivity reached 0.26 nm/° (7.45 nm/(rad/m)). Though responses to both directions are the same, because the fiber showed wide response range, in practice pre-twist can be set in order to realize dual twist direction discrimination at the expense of narrowing measurement range.

B. Temperature compensating

Then the fiber sample was coiled into laps and put in a thermal chamber, we did not carry out simultaneous twist test at different temperatures limited by the size of chamber, the aim of this section was to investigate how much temperature influences and produce a plan to compensate. Envelopes were tracked as temperature varying. As temperature increased, the dips of lower envelope blue shifted. We speculate that, because the cores are scattered in different positions in fiber, they suffer uneven thermal expansion of the silica, since core 1 is in the center and well-covered by surrounding silica glass, it expanded the most among three cores, while core 3 is the outermost and the covering silica glass is thinner, therefore it expanded the least. Phase differences reduced because of this and caused blue shift of the spectrum. Temperature response was recorded every 10 °C as temperature slowly cooling down from 70 °C to room temperature of 20 °C, the outlined envelope shifted about 13 nm, which is shown in Fig. 7. The inset is the linear fitting result which indicate the temperature

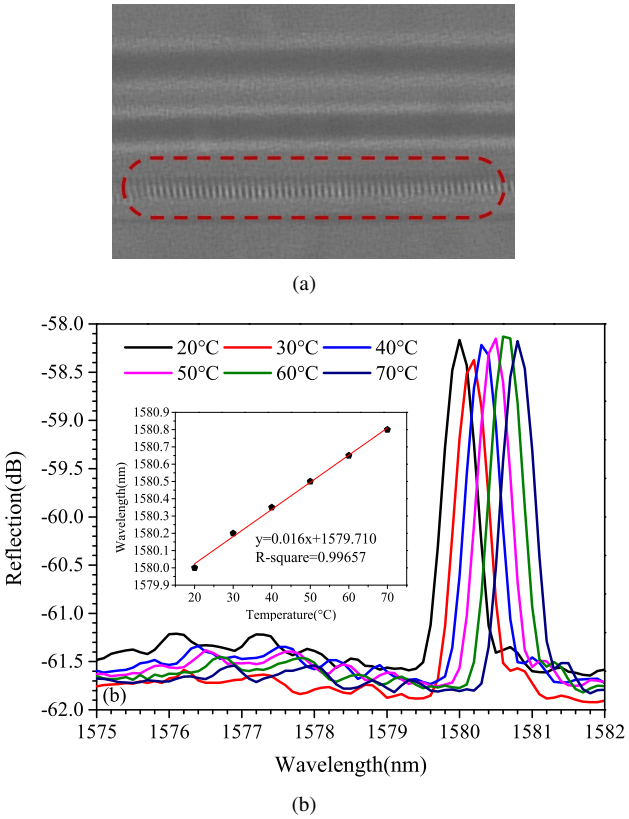

Fig. 8. (a) To compensate the influence of temperature, an FBG was written on a core with femtosecond laser. (b) The temperature response of the FBG (Inset: linear fitting of the relation between Bragg wavelength and temperature).

sensitivity is -0.26 nm/°C. This value, however, is not low enough so the influence of temperature cannot be neglected. To compensate this factor, a section of FBG was inscribed on core 1 which has the least deformation under torsion with femtosecond laser (520 nm, 10 kHz) (Fig. 8(a)). The grating is extremely short, which is only ∼1 mm in length, it is insensitive to twist and it does not influence the twist sensing characteristics of the MZI. Because the Bragg wavelength is covered by numerous dips in transmission spectrum and uneasy to track, reflection spectrum of the grating was observed with a circulator. The Bragg wavelength is at ∼1580 nm. The reflection peak will shift with varying temperature due to thermo-optic effect which influences the refractive indices and material thermal expansion which alters the period. Fig. 8(b) illustrates the Bragg wavelength at different temperature, and the FBG temperature sensitivity was 0.016 nm/°C. Both the 3CF MZI and the FBG temperature responses are in high linearity, temperature influence on sensing can be compensated in this way. The real envelope dips shift caused by twist can be calculated by $\Delta\lambda_{twist} = \Delta\lambda + 0.26\Delta T$. Temperature compensated by FBG is a very common method, it is effective, highly linear, and moreover in this case, it is well integrated since the FBG was directly inscribed on the 3CF.

IV. Conclusion

The eccentric 3CF was introduced in this paper. The fabrication of this 3CF is relatively easy. Because of the asymmetric

distribution of the three cores, twist sensing can be realized based on the principle that inducing phase differences in beams due to unequal stretches among the cores to form Mach-Zehnder interference. The total output spectrum consists of three interference components and evolves into envelopes. The lower envelope dips shift were tracked and the response to twist angle were quadratic, sensitivity becomes higher as twist accumulate. The sample had sensitivity of 7.45 nm/(rad/m) from 540° to 720°, it can be considered linear in this limited range. Sensitivity will continue increasing if the fiber is further twisted. The response to both twisting directions are identical, so pre-twist is necessary to realize direction discrimination. This fiber is suitable for twist measurement in engineering, industrial or architecture for its high sensitivity and wide response range, it is also easy-configuration and low costing.

REFERENCES

[1] A. Barrias, J. Casas and S. Villalba, A Review of distributed optical fiber sensors for civil engineering applications, Sensors-Basel, vol. 16, no. 5, 748, 2016.

[2] J. Li, H. Yan, H. Dang and F. Meng, Structure design and application of hollow core microstructured optical fiber gas sensor: A review, Opt. Laser Technol, vol. 135, 106658, 2021.

[3] S. Mihailov, Fiber Bragg grating sensors for harsh environments, Sensors-Basel, vol. 12, no.2, pp. 1898-1918, 2012.

[4] H. Joe, H. Yun, S. Jo, M. Jun and B. Min, A review on optical fiber sensors for environmental monitoring, Int. J. Precis Eng Manuf-Green Technol., vol.5, no. 1, pp. 173-191, 2018.

[5] C. Davis, S. Tejedor, I. Grabovac, J. Kopczyk, and T. Nuyens, Highstrain fiber Bragg gratings for structural fatigue testing of military aircraft, Photonic Sensors, vol. 2, no. 3, pp. 215-224, 2012.

[6] C.-C. Zhang, H.-H. Zhu, and B. Shi, Role of the interface between distributed fibre optic strain sensor and soil in ground deformation measurement, Sci. Rep., vol. 6, no. 1, 36469, 2016.

[7] M. Iten, A. M. Puzrin, and A. Schmid, Landslide monitoring using a road-embedded optical fiber sensor, Proc. SPIE, vol. 6933, 2008.

[8] X. Chen, K. Zhou, L. Zhang, and I. Bennion, In-Fiber twist sensor based on a fiber Bragg grating with 81° tilted structure. IEEE Photonic Technol. Lett., vol. 18, no. 24, pp. 2596-2598, 2006.

[9] Y. Lu, C. Shen, D. Chen, J. Chu, Q. Wang, and X. Dong, Highly sensitive twist sensor based on tilted fiber Bragg grating of polarization-dependent properties Opt. Fiber Technol., vol. 20, pp. 491-494, 2014.

[10] Y. Wang, M. Wang and X. Huang, In fiber Bragg grating twist sensor based on analysis of polarization dependent loss, Opt. Express, vol. 21, no. 10, 11913, 2013.

[11] C. Shen, Z. Yang, W. Zhou and J. Albert, Au-coated tilted fiber Bragg grating twist sensor based on surface plasmon resonance, Appl. Phys. Lett. vol. 104, 071106, 2014.

[12] R. Gao, Y. Jiang, and L. Jiang, Multi-phase-shifted helical long period fiber grating based temperature-insensitive optical twist sensor, Opt. Express, vol. 22, no. 13, 15697 2014.

[13] Y. Zhao, S. Liu, J. Luo, Y. Chen, C. Fu, C. Xiong, Y. Wang, S. Jing, Z. Bai, C. Liao, and Y. Wang, torsion, refractive index, and temperature sensors based on an improved helical long period fiber grating, IEEE J. Lightwave Technol., vol. 38, no. 8, pp. 2504-2510, 2020.

[14] P. Zu, C. Chan, Y. Jin, T. Gong, Y Zhang, L. Chen, and X. Dong, A temperature-insensitive twist sensor by using low-birefringence photonic-crystal-fiber-based Sagnac interferometer, IEEE Photonics Technol. Lett. vol. 23, no.13, pp. 920-922, 2011.

[15] Y. Chen, Y. Semenova, G. Farrell, F. Xu, and Y. Lu, A compact Sagnac loop based on a microfiber coupler for twist sensing. IEEE Photonics Technol. Lett., vol. 27, no. 24, pp. 2579-2582, 2015.

[16] L. Shao, X. Zhang, H. He, Z. Zhang, X. Zou, B. Luo, W. Pan and L. Yan. Optical fiber temperature and torsion sensor based on Lyot-Sagnac interferometer, Sensors-Basel, vol. 16, 1774, 2016.

[17] H. Liang, M. Sun and Y. Jin, Twist sensor based on Sagnac single-mode optic fiber interferometer. Optik, vol. 124, pp. 6676-6678, 2013.

[18] B. Huang and X. Shu, Highly sensitive twist sensor based on temperature- and strain-independent fiber Lyot filter. IEEE J. Lightwave Technol. vol. 35, no. 10, pp. 2026-2031, 2017.

[19] T. Yuan, X. Zhang, Q. Xia, Y. Wang, and L. Yuan, Design and fabrication of a functional fiber for micro flow sensing, IEEE J. Lightwave Technol. vol. 39, no. 1, pp. 290-294, 2021.

[20] E. Chillcce, C. Cordeiro, L. Barbosa and C. Cruz, Tellurite photonic crystal fiber made by a stack-and-draw technique, J. Non-Cryst. Solids, vol. 352, 32-35, pp. 3423-3428, 2006.

[21] E. Chillcce, C. Cordeiro, R. Ramos, B. Honrio, E. Rodriguez, G. Jacob, C. Cruz, C. Cesar and L. Barbosa, Development of soft-glasses photonic crystal fiber made by stacking-and-draw technique, Optical Components and Materials IV, vol. 6469, 64690U, 2017.

[22] J. Liou and C. Yu, All-fiber Mach-Zehnder interferometer based on two liquid infiltrations in a photonic crystal fiber. Opt. Express, vol. 23, no. 5, pp. 6946-6951, 2015.

[23] S. Yan, Y. Zhao, M. Chen and Q. Liu, Optical fiber strain sensor with double S-tapers. Instrum. Sci. Technol., vol. 49, no. 3, pp. 313-326, 2021.

Pingsheng Xue received the B.S. degree from the College of Electrical Engineering, Yanshan University, China, in 2019. He is currently pursuing the master's degree with the College of Control Engineering, Northeastern University at Qinhuangdao, Qinhuangdao, China.

Qiang Liu received the B.S. and Ph.D. degrees from the College of Science, Yanshan University, China, in 2013 and 2018, respectively. He studied in Northeastern University, Shenyang, China from March 2015 to July 2015 as a visiting student. He is a Lecturer working in the School of Control Engineering, Northeastern University at Qinhuangdao, China. In 2018, he was awarded "Outstanding Graduate of Hebei Province, China". In 2019, he was awarded "Excellent Doctoral Thesis of Hebei Province, China". In 2020, he has been a Supervisor of Master in Northeastern University, China. From January 2020 to March 2021, he was a Postdoctor with Faculty of Engineering and Environment, Northumbria University, Newcastle Upon Tyne, United Kingdom. His research interests include fiber optical sensors, fiber modulators, polarization filters, fiber splitters, functional materials, smart materials, photonic crystal fibers and their applications. He has authored and co-authored more than 50 scientific papers.

Qiang Wu received the B.S. and Ph.D. degrees from Beijing Normal University and Beijing University of Posts and Telecommunications, Beijing, China, in 1996 and 2004, respectively. From 2004 to 2006, he worked as a Senior Research Associate in City University of Hong Kong. From 2006 to 2008, he took up a research associate post in Heriot-Watt University, Edinburgh, U.K. From 2008 to 2014, he worked as a Stokes Lecturer at Photonics Research Centre, Dublin Institute of Technology, Ireland. He is an Associate Professor/Reader with Faculty of Engineering and Environment, Northumbria University, Newcastle Upon Tyne, United Kingdom. His research interests include optical fiber interferometers for novel optical couplers, nanofibers and sensors, microsphere sensors for bio-chemical sensing, the design and fabrication of fiber Bragg grating devices and their applications for sensing, nonlinear fibre optics, surface plasmon resonant and surface acoustic wave sensors. He has over 200 publications in the area of photonics and holds 3 invention patents. He is an Editorial Board Member of Scientific Reports, Associate Editor of IEEE

Sensors Journal and Academic Editor of Journal of Sensors.

Yongqing Fu received the Ph.D. degree from Nanyang Technological University in 1999, Singapore, and then worked as a Research Fellow in Singapore-Massachusetts Institute of Technology Alliance, and a Research Associate in University of Cambridge. He is currently a Professor at Northumbria University, UK. He was a Reader in Thin Film Centre in University of West of Scotland, Glasgow, UK, and a lecturer in Heriot-Watt University, Edinburgh, UK. He has extensive experience in smart thin film/materials, biomedical microdevices, energy materials, lab-on-chip, micromechanics, MEMS, nanotechnology, sensors and microfluidics. He has established a worldwide reputation from his pioneer research work on shape memory films, piezoelectric thin films, nanostructured composite/films for applications in MEMS, sensing and renewable energy applications. He has authored and co-authored about 150 refereed international journal papers, one book on thin film shape memory alloys and ten book chapters in these areas. He has been regularly invited as referees for over 30 different international journals, and serves as editorial board member for three international journals.